Exploring the relationship between predicted negative energy balance and its biomarkers of Holstein cows in first-parity early lactation

Hongqing Hu,[1] ⓘ Sébastien Franceschini,[1] ⓘ Pauline Lemal,[1] ⓘ Clément Grelet,[2] ⓘ Yansen Chen,[1] ⓘ Hadi Atashi,[1] ⓘ Katrien Wijnrocx,[1] ⓘ Hélène Soyeurt, [1] ⓘ and Nicolas Gengler[1]* ⓘ
[1]TERRA Teaching and Research Center, University of Liège, Gembloux Agro-Bio Tech (ULiège-GxABT), 5030 Gembloux, Belgium
[2]Walloon Agricultural Research Center (CRA-W), 5030 Gembloux, Belgium

ABSTRACT

The negative energy balance (NEB) state in dairy cows is a critical factor affecting health, reproduction, and production, particularly during early lactation. Multiple blood and milk biomarkers change when dairy cows are in the NEB state. Direct measurement of NEB is impractical for large-scale use due to costs, necessitating reliance on indirect predictors such as milk mid-infrared (MIR) spectrometry-based predicted biomarkers. However, the genetic relationships between NEB and its potential biomarkers remain unclear. This study aimed to (1) compare measured reference NEB with MIR-predicted NEB (PNEB), a novel energy deficit score (EDS), 15 biomarkers, and 3 production traits; (2) estimate genetic parameters among these traits using a 20-trait repeatability model, quantifying the ability of the 19 other studied traits (logit-transformed EDS (LEDS), 15 biomarkers, and 3 production traits) to genetically predict logit-transformed PNEB (LPNEB); and (3) evaluate the causal effects of LPNEB on the 19 traits through a recursive model. Two datasets were used: dataset I (127 cows, 965 records) provided reference data for objective (1), and dataset II (25,287 first-parity cows, 30,634 records) enabled genetic analysis used for objectives (2) and (3). Traits were analyzed using Pearson correlations, multiple-diagonalization expectation maximization REML–based genetic parameter estimation, and recursive modeling. The studied traits had moderate to moderate-high h^2 ranging from 0.16 to 0.38. The genetic correlations between LPNEB and the studied traits ranged from −0.60 for LIGF-1 to 0.85 for MIR-predicted blood nonesterified fatty acids (NEFA). Analysis of genetic predictability of LPNEB traits together explained 89% of the genetic variance of LPNEB, with all 15 biomarkers alone contributing the largest fraction with 82%, LEDS alone 65%, NEFA alone 62%, and all traits except LEDS 85%, indicating that LEDS contains useful additional information. Recursive modeling further identified 8 traits, including NEFA and LEDS, as highly dependent on LPNEB, highlighting their potential as robust biomarkers. This study demonstrates the utility of MIR-predicted traits for understanding the genetic mechanisms of NEB and its potential for integration into breeding programs, while emphasizing cautious interpretation of these results due to limitations of MIR-predictions of studied traits to represent directly measured traits.

Key words: milk mid-infrared, genetic correlation, phenotypic correlation, recursive model

INTRODUCTION

Energy balance (**EB**) in dairy cows refers to the difference between the energy intake and the energy expended for maintenance and production activities, such as milk production, growth, and reproduction (Baumgard et al., 2006). In the early lactation stage, when the energy intake cannot meet the demands of milk production, most dairy cows are in the state of negative EB (**NEB**; Churakov et al., 2021). For example, a recent study considered that 75.2% of cows in the UK were in NEB during the first 20 DIM (Macrae et al., 2019). Other studies have shown that the extent and duration of the postpartum NEB state is an important factor affecting the reproduction and health of dairy cows (Collard et al., 2000). If a dairy cow stays in the NEB state for a long period, the risk of metabolic diseases (e.g., ketosis) will increase. In addition, the NEB state is associated with decreased conception rates, increased early embryo mortality, and increased estrus silencing in dairy cows (Zachut et al., 2020).

Monitoring the occurrence of the NEB state in dairy cows in early lactation is essential for optimizing the health condition of dairy herds (Churakov et al., 2021) and generating data for breeding purposes for reduced NEB risk. Although metabolic chambers are the gold standard method for detecting energy status, this equip-

The list of standard abbreviations for JDS is available at adsa.org/jds-abbreviations-25. Nonstandard abbreviations are available in the Notes.

ment is too expensive for large-scale applications (Churakov et al., 2021). There are a few reports with a very small number of records on the genetic analysis of measured EB (e.g., Berry et al., 2007; Liinamo et al., 2012). Moreover, BCS has traditionally been used to monitor animals and identify those that are in NEB (Stádník et al., 2002). However, human-assessed BCS scores are subjective, labor-intensive, and not easily available as repeated records in early lactation. Also, even if precision livestock farming tools based on computer vision are becoming available, these technologies remain expensive and are not easy to implement in commercial farms. Therefore, the development of an objective, accurate, quick, inexpensive, and easy procedure to detect NEB in dairy farms is still needed.

For dairy cows, being in an NEB state is a complex physiological metabolic process involving multiple changes in the metabolic pathways and energy sources, modifying blood content of nonesterified fatty acid (**NEFA**), β-hydroxybutyrate acid (**BHBA**), or IGF-1 (Xu et al., 2020; Zachut et al., 2020; Pires et al., 2022). Therefore, when testing NEB on farms, veterinarians traditionally rely on directly measured levels of these biomarkers (Macrae et al., 2019). However, direct measuring of these biomarkers is always based on blood samples that are obtained in an invasive manner, which is not recommended on a large scale for animal welfare reasons. Furthermore, for practical reasons, most studies used only 1 or 2 biomarkers, such as NEFA or BHBA, for predicting an NEB state. These 2 issues could potentially be addressed using milk mid-infrared (**MIR**) spectrometry-based predictions. Indeed, several suitable predictors using milk MIR spectrometry, which is obviously a noninvasive method, for milk but also blood biomarkers have been reported (Grelet et al., 2021). However, some biomarkers remain potentially poorly predicted by MIR spectrometry. Therefore, recently, Franceschini et al. (2022) used an unsupervised machine-learning method to integrate multiple biomarkers (mostly MIR-predicted biomarkers) into a clustering approach to develop a novel trait called hereafter the energy deficit score (**EDS**).

Mid-infrared spectrometric data are used to predict several biomarkers and can be considered to be an efficient approach to predict EB in dairy cows as well. However, as already stated, the coefficients of determination of the different prediction models vary across studies (from 0.48 to 0.78; McParland and Berry, 2016; Smith et al., 2019; Ho et al., 2020), indicating that not all biomarkers can be predicted in a reliable manner using MIR spectrometry. McParland et al. (2015) and Smith et al. (2019) reported genetic parameters of MIR-predicted EB with larger datasets. However, in all these studies, the genetic relationships between NEB state and multiple biomarkers and economically relevant traits, for example, production traits such as fat percentage (**FP**), protein percentage (**PP**), and milk yield (**MY**) remain unclear.

The objectives of this study were therefore to (1) compare measured reference NEB (**RNEB**) to MIR-predicted NEB (**PNEB**), EDS, 15 biomarkers, and 3 production traits; (2) estimate the genetic parameters among the mentioned traits using a 20-trait repeatability model allowing the quantification of the ability of the 19 other traits (i.e., biomarkers) to genetically predict the logit-transformed predicted NEB (**LPNEB**); (3) use these genetic parameters to estimate the causal effects of LPNEB on the 19 mentioned traits through a recursive model. Achieving these objectives will allow the highlighting of the role of other traits (i.e., biomarkers) in predicting NEB, as well as the causal effects of NEB on other traits. However, due to the reliance on MIR-predicted traits in this study, conclusions will be drawn cautiously to avoid overinterpretation.

MATERIALS AND METHODS

Data Collection and Editing

Because this study used many MIR-predicted biomarkers in a first step, we used a dataset I, which included RNEB, PNEB, and 19 other traits. Dataset I allowed us to compare observed correlations of RNEB with PNEB and the other 19 traits. It was collected by the GplusE Project (https://gpluse.eaap.org/) on 3 experimental farms located in 3 different countries (Agri-Food and Biosciences Institute, Belfast, UK; Aarhus University, Aarhus, Denmark; and University College Dublin, Dublin, Ireland). This dataset provided access to 1,033 directly measured reference EB (**REB**) records on 129 dairy cows collected from 5 to 50 DIM. The diet of the animals and the analysis methods have been previously reported by Grelet et al. (2020). In a second part of the study, a larger dataset (including 20 traits) was used to do genetic analysis, hereafter referred to as dataset II. We used dataset II to calculate the genetic relationships among 20 traits, revealing their genetic components and interrelationships. Dataset II was compiled during the official recording of milk data in the Walloon Region of Belgium from 2012 to 2019. Both datasets encompassed the same 20 traits, except for REB, which was exclusively included in dataset I. Please note that to distinguish directly measured biomarkers from those predicted by MIR spectrometry, abbreviations will be employed solely for the MIR-predicted biomarkers. The considered traits (n = 20) in both datasets include predicted EB (**PEB**), EDS, 15 biomarkers, and 3 production traits (FP, PP, MY). The choice of the 15 biomarkers was based on their recognized involvement in energy metabolism. The PEB and

Table 1. Description of the 16 traits[1] prediction equations used in this study

Trait	Unit	R^2cv[2]	RMSEcv[3]	Reference
EB	Mcal/d	0.43	NA[4]	Grelet et al., 2017
In blood				
B_BHBA	mmol/L	0.70	0.27	Grelet et al., 2019
NEFA	µekv/L	0.39	344.20	Grelet et al., 2019
IGF-1	mg/L	0.61	44.40	Grelet et al., 2019
GLU	mmol/L	0.44	0.36	Grelet et al., 2019
In milk				
M_BHBA	mmol/L	0.71	0.11	Grelet et al., 2016
CIT	mmol/L	0.90	0.70	Grelet et al., 2016
ACE	mmol/L	0.73	0.25	Grelet et al., 2016
C10:0	g/dL of milk	0.91	0.09	Soyeurt et al., 2006
C14:0	g/dL of milk	0.93	0.07	Soyeurt et al., 2006
C16:0	g/dL of milk	0.94	0.08	Soyeurt et al., 2006
C18:0	g/dL of milk	0.84	0.14	Soyeurt et al., 2006
C18:1 *cis*-9	g/dL of milk	0.95	0.08	Soyeurt et al., 2011
SCFA	g/dL of milk	0.93	0.07	Soyeurt et al., 2011
MCFA	g/dL of milk	0.97	0.05	Soyeurt et al., 2011
LCFA	g/dL of milk	0.95	0.07	Soyeurt et al., 2011

[1]EB = energy balance; B_BHBA = blood β-hydroxybutyric acid; NEFA = blood nonesterified fatty acids; GLU = blood glucose; M_BHBA = milk β-hydroxybutyric acid; CIT = milk citrate; ACE = milk acetone; C10:0 = milk decanoic acid; C14:0 = milk myristic acid; C16:0 = milk palmitic acid; C18:0 = milk stearic acid; C18:1 *cis*-9 = milk oleic acid; SCFA = milk short-chain fatty acids; MCFA = milk medium-chain fatty acids; LCFA = milk long-chain fatty acids.

[2]R^2cv = coefficient of determination of cross-validation.

[3]RMSEcv = root mean square error of cross-validation.

[4]NA = not applicable because data were not available.

the selected biomarkers (n = 15) were predicted by milk MIR spectrometry or MIR spectra data plus MY and parity. All the used prediction equations were described in previous publications as outlined in Table 1. Milk MIR spectra, FP, and PP were generated by commercial instruments FT2, FT6000 spectrometers (Foss Analytics) and on a Standard Lactoscope FT-MIR automatic (Delta Instruments). Mid-infrared spectral data of the 2 datasets were standardized by the method proposed by Grelet et al. (2015). Milk yield was recorded during milk sampling. As described by Franceschini et al. (2022), the EDS trait was defined using the agglomerative hierarchical clustering method based on 27 MIR-based predictors. However, new observations were predicted directly using MIR spectral data. More details on the methodology and the 27 MIR spectra-based predictors can be found in Franceschini et al. (2022).

Trait Transformations. Because PEB does not reflect the relative risk of being in an NEB predicted from MIR spectral data (PNEB), PEB was converted into PNEB by the following formula:

$$PNEB = 1 - \frac{PEB - PEB_{minimum}}{PEB_{maximun} - PEB_{minimum}}$$, expressing NEB

as a relative value in the observed range of PEB values in a given dataset. The larger the value of PNEB, the worse the energy status of the cow expressed on this relative scale. The probabilities of PNEB and EDS were subjected to a logit-like transformation due to their nonnormal distribution because they were constrained within the interval of 0 to 1. The formula employed for calculating PNEB is expressed as follows: LPNEB = $\log_{10}$[PNEB/(1 − PNEB)]. To ensure that the values of PNEB remained within a specified range, those below 0.001 were adjusted to 0.001, and those exceeding 0.999 were set to 0.999. This adjustment effectively confines the range of LPNEB to between −3 and +3. The same procedure was used for measured REB generating logit-transformed measured reference NEB (**LRNEB**). These transformations notably enhanced the theoretical properties of LPNEB and LRNEB compared with those of PEB and measured REB, by expressing better relative risk under the specific production circumstances of each dataset. However, this improvement came at the cost of losing the ability of direct comparisons of descriptive parameters, particularly the means of these traits, across variables and datasets. An equivalent formula was then used to compute and to define a novel logit-like transformed EDS (**LEDS**): LEDS = $\log_{10}$[EDS/(1 − EDS)]. These transformations are related to odds as a way of expressing the likelihood of an event (here risk of NEB state) occurring compared with it not occurring. Using base 10 facilitated the treatment of extreme boundaries, here to be set between −3 and +3, and does not affect results. Therefore, in further text the used transformation will be called logit-transformation.

The visual inspection showed MIR-based predictions of blood β-hydroxybutyric acid (**B_BHBA**), IGF-1, milk β-hydroxybutyric acid (**M_BHBA**), and acetone (**ACE**) to deviate from a normal distribution (Figure 1). Therefore, $\log_{10}$ transformations were applied (**LB_BHBA**, **LIGF-1**, **LM_BHBA**, **LACE**) leading to distributions that were closer to normal (Figure 1). As a reminder, we are using abbreviations of biomarker names only for the MIR-based predictions.

Data Editing. All the following procedures were applied to both datasets. Milk yield, FP, and PP were limited from 3 to 99 kg/day, 1% to 9%, and 1% to 7%, respectively (ICAR, 2022). The filter proposed by Chen et al. (2021) was used for cleaning the selected milk MIR-predicted traits (PNEB and 15 biomarkers in blood and milk). The global H distances (Whitfield et al., 1987) were computed for each standardized MIR spectrum in this study in relation to the MIR spectra from the calibration dataset corresponding to the various traits. Only those MIR records with a global H value of 3 or less were retained. Furthermore, all predicted traits were constrained within a DIM range of 5 to 50 because the predictive models for certain biomarkers are exclusively applicable within this DIM range (e.g., PEB, B_BHBA).

Used Datasets and Traits. A total of 965 data records on 127 Holstein cows (with parity levels varying from 1 to 7, mean: 2.75, SD: 1.54) across 3 herds were retained for dataset I. Additionally, dataset II consisted of 30,634 records from 25,287 first-parity Holstein cows distributed in 508 herds. The pedigrees for the animals included in dataset II were sourced from the Walloon genetic evaluation system, which incorporated 4 generations of ancestors, culminating in a total of 74,662 animals, including 4,700 bulls.

The studied traits were LRNEB (only dataset I), LPNEB, LEDS, 15 biomarkers including LB_BHBA, NEFA, LIGF-1, glucose (**GLU**), LM_BHBA, citrate (**CIT**), LACE, decanoic acid (**C10:0**), myristic acid (**C14:0**), palmitic acid (**C16:0**), stearic acid (**C18:0**), short-chain fatty acids (**SCFA**), medium-chain fatty acids (**MCFA**), long-chain fatty acids (**LCFA**), oleic acid (**C18:1 cis-9**), and 3 production traits (FP, PP, MY).

Comparison of Measured EB and Predicted EB with 19 Other Traits

To examine the associations between LPNEB (LRNEB for dataset I) and the remaining 19 traits, Pearson correlations (r) and their corresponding *P*-values were computed for both datasets. This approach was considered essential because dataset I was too limited in size to support a robust genetic analysis.

To eliminate the influence of parity on traits in dataset I, we applied a linear model to adjust traits, standardizing them to the baseline level of parity 1. The specific approach is as follows. First inside a given trait a linear model for each observation i inside parity class ($y_{ij} = \beta_j + \varepsilon_{ij}$) was constructed based on the parity classification variable, and the solution corresponding to parity 1, here β_1 was extracted. The adjusted trait value for y_{ij} $\left(y_{ij}^{\text{adjusted}}\right)$ was then calculated using the formula: $y_{ij}^{\text{adjusted}} = y_{ij} - \beta_j + \beta_1$, where β_j represents the predicted value from the model and β_1 represents the effect of parity 1. The adjusted trait values, labeled as "adjusted traits" are corrected to the level of parity 1, ensuring theoretical consistency when comparing traits across different parities.

Genetic Parameters Estimation

(Co)variance Component Estimation. The estimation of (co)variance components for 20 traits within dataset II was conducted using a 20-trait repeatability model. This approach was facilitated by the application of canonical transformation across multiple matrices, employing the multiple-diagonalization method as described by Misztal et al. (1995) using the following model:

$$\mathbf{y} = \mathbf{Hh} + \mathbf{Mm} + \mathbf{Cc} + \mathbf{Dd} + \mathbf{Qq} + \mathbf{Wp} + \mathbf{Za} + \mathbf{e},$$

where $\mathbf{y}$ is the vector of observations for the studied traits (n = 20: LPNEB, LEDS, 15 biomarkers, and 3 production traits); $\mathbf{h}$ is the vector of fixed effect for herd × calving year; $\mathbf{m}$ is the vector of fixed effect of calving age (10 classes: 23–24 mo, 25, 26, 27, 28, 29, 30, 31–32 mo, 33–34 mo, and 35–37 mo); $\mathbf{c}$ is the vector of fixed effect for calving month (12 class month); $\mathbf{d}$ is the fixed vector of DIM classes (classes: DIM 5–6, 7–8, 9–10, and 11–50); $\mathbf{q}$ is the fixed regression coefficient vector of standardized DIM, and its quadratic, $\mathbf{p}$ is the vector of the random permanent environmental effects, $\mathbf{a}$ is the vector of random additive genetic effects; $\mathbf{e}$ is the vector of residual effects. Additionally, $\mathbf{H}$, $\mathbf{M}$, $\mathbf{C}$, $\mathbf{D}$, $\mathbf{Q}$, $\mathbf{W}$, and $\mathbf{Z}$ are incidence matrices. Both classes and regressions were used to model the very rapid changes of certain biomarkers at the beginning of lactation and goodness of fit obtained by visually comparing mean values of traits with sums of class and regression effects at each DIM.

The expected values and variances associated with this model were defined as follows:

$$E(\mathbf{y}) = \mathbf{Hh} + \mathbf{Mm} + \mathbf{Cc} + \mathbf{Dd} + \mathbf{Qq}, E(\mathbf{p})$$
$$= E(\mathbf{a}) = E(\mathbf{e}) = \mathbf{0}.$$

The matrices Var($\mathbf{p}$) and Var($\mathbf{a}$) contained 20 × 20 basic (co)variance blocks among the 20 traits. For Var($\mathbf{e}$), the
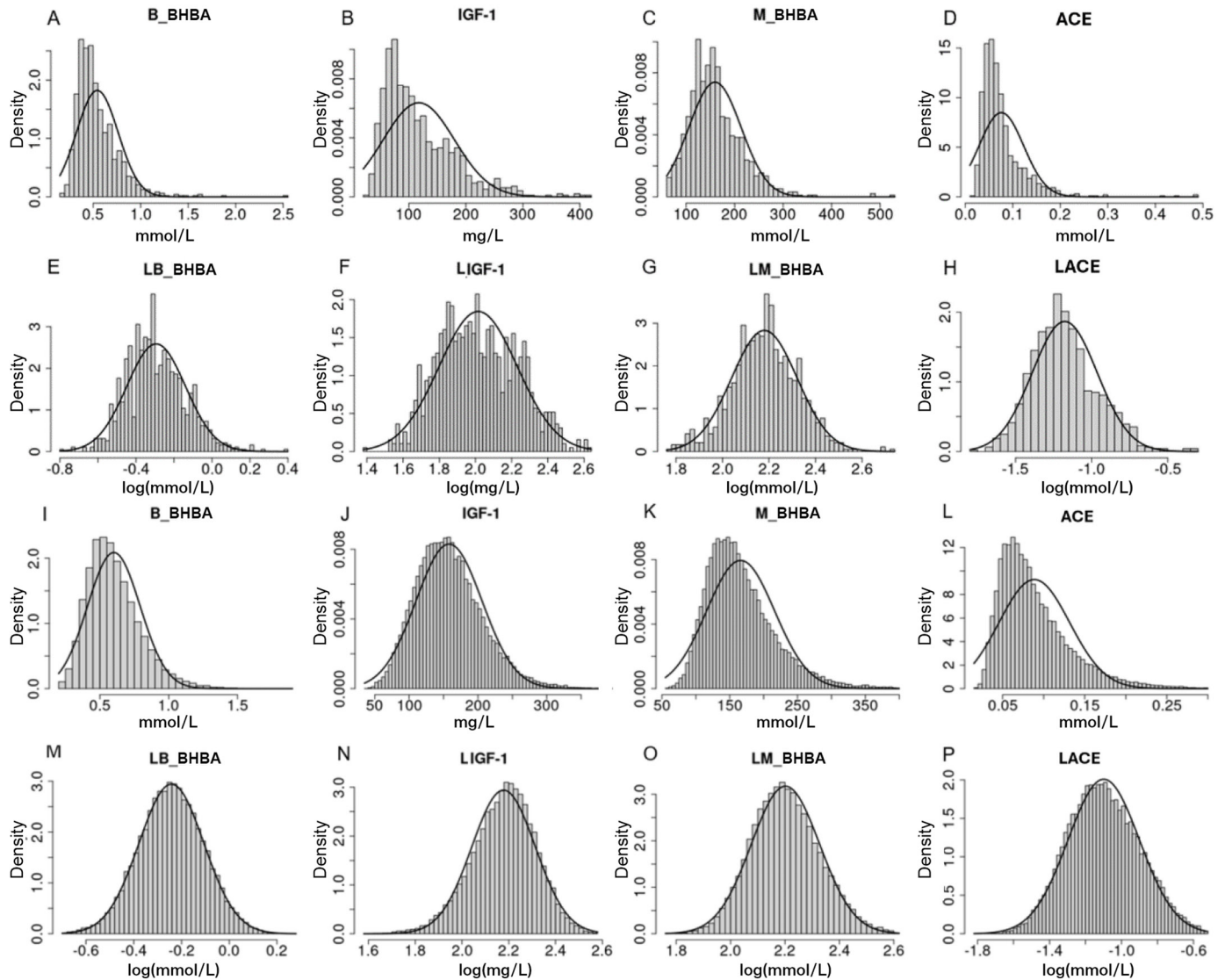
Figure 1. Distribution of the standardized 16 traits in dataset I (A–H) and dataset II (I–P). (A) Blood β-hydroxybutyric acid predicted by mid-infrared spectra; (B) blood IGF-1 predicted by mid-infrared spectra; (C) milk β-hydroxybutyric acid predicted by mid-infrared spectra; (D) milk acetone predicted by mid-infrared spectra; (E) log_{10} blood β-hydroxybutyric acid predicted by mid-infrared spectra; (F) log_{10} blood IGF-1 predicted by mid-infrared spectra; (G) log_{10} milk β-hydroxybutyric acid predicted by mid-infrared spectra; (H) log_{10} milk acetone predicted by mid-infrared spectra; (I) blood β-hydroxybutyric acid predicted by mid-infrared spectra; (J) blood IGF-1 predicted by mid-infrared spectra; (K) milk β-hydroxybutyric acid predicted by mid-infrared spectra; (L) milk acetone predicted by mid-infrared spectra; (M) log_{10} blood β-hydroxybutyric acid predicted by mid-infrared spectra; (N) log_{10} blood IGF-1 predicted by mid-infrared spectra; (O) log_{10} milk β-hydroxybutyric acid predicted by mid-infrared spectra; (P) log_{10} milk acetone predicted by mid-infrared spectra.

off-diagonal elements were modeled as nonzero values, representing residual covariance between correlated traits. This approach ensures that the environmental covariance among traits is not concentrated on the permanent environmental effects.

Due to the informative pedigree, genetic and permanent environmental effects could be separated. Given the fact that we needed reliable (co)variance components for 20 traits, a fast and robust expectation maximization REML (**EM-REML**) algorithm was used that integrated the multiple-diagonalization algorithm as implemented by Misztal et al. (1995) in the MTC program (http://nce .ads.uga.edu/~ignacy/numpub/mtc/mtcman). This MTC program was shown to be adapted for situations where many (co)variances had to be estimated at the same time (e.g., Rustin et al., 2009) using deceleration during (co)variance components updating as first proposed by Wiggans et al. (2006). Computing time for a round of EM-REML estimation was approximately 20 times faster when using multiple diagonalization. Relative

Table 2. Mean and SD values for the 21 traits[1] used in datasets I and II

| Trait | Unit | Dataset I | | | | | | Dataset II | |
| | | 1st parity (n = 243) | | All parities (n = 965) | | Adjusted to 1st parity (n = 965) | | 1st parity (n = 30,634) | |
		Mean	SD	Mean	SD	Mean	SD	Mean	SD
LRNEB	na[2]	−0.03	0.28	0.09	0.31	−0.03	0.30	NA[3]	NA
LPNEB	na	−0.50	0.35	−0.30	0.35	−0.50	0.31	−0.09	0.29
LEDS	na	−0.57	0.15	−0.59	0.15	−0.57	0.15	−0.53	0.16
In blood									
LB_BHBA	log(mmol/L)	−0.33	0.15	−0.29	0.15	−0.33	0.15	−0.24	0.14
NEFA	μekv/L	490.97	277.42	546.23	244.56	490.97	242.30	474.36	225.22
LIGF-1	log(mg/L)	2.19	0.17	2.01	0.22	2.19	0.17	2.18	0.14
GLU	mmol/L	3.83	0.25	3.65	0.25	3.83	0.22	3.72	0.21
In milk									
LM_BHBA	log(mmol/L)	2.21	0.11	2.18	0.14	2.21	0.14	2.20	0.13
CIT	mmol/L	8.80	1.30	9.06	1.69	8.80	1.68	8.88	1.45
LACE	log(mmol/L)	−1.15	0.22	−1.18	0.21	−1.15	0.21	−1.10	0.20
C10:0	g/dL of milk	0.09	0.02	0.10	0.02	0.09	0.02	0.09	0.02
C14:0	g/dL of milk	0.42	0.08	0.44	0.08	0.42	0.08	0.40	0.07
C16:0	g/dL of milk	1.22	0.22	1.22	0.24	1.22	0.24	1.10	0.20
C18:0	g/dL of milk	0.51	0.09	0.51	0.10	0.51	0.10	0.48	0.09
C18:1 cis-9	g/dL of milk	0.89	0.22	0.87	0.24	0.89	0.23	0.91	0.23
SCFA	g/dL of milk	0.34	0.06	0.35	0.06	0.34	0.06	0.32	0.06
MCFA	g/dL of milk	1.93	0.34	1.96	0.36	1.93	0.36	1.77	0.30
LCFA	g/dL of milk	1.82	0.39	1.80	0.40	1.82	0.40	1.81	0.38
FP	% milk	4.00	0.54	4.00	0.61	4.00	0.60	3.79	0.54
PP	% milk	3.18	0.31	3.14	0.31	3.18	0.31	3.13	0.29
MY	kg/d	25.32	6.54	35.58	9.37	25.32	7.10	26.94	5.33

[1] LRNEB = logarithm measured probability NEB; LPNEB = logarithm probability NEB predicted by mid-infrared spectra; LEDS = logarithm probability EDS; LB_BHBA = log$_{10}$ blood β-hydroxybutyric acid predicted by mid-infrared spectra; NEFA = blood nonesterified fatty acids predicted by mid-infrared spectra; LIGF-1 = log$_{10}$ blood IGF-1 predicted by mid-infrared spectra; GLU = blood glucose predicted by mid-infrared spectra; LM_BHBA = log$_{10}$ milk β-hydroxybutyric acid predicted by mid-infrared spectra; CIT = milk citrate predicted by mid-infrared spectra; LACE = log$_{10}$ milk acetone predicted by mid-infrared spectra; C10:0 = milk decanoic acid predicted by mid-infrared spectra; C14:0 = milk myristic acid predicted by mid-infrared spectra; C16:0 = milk palmitic acid predicted by mid-infrared spectra; C18:0 = milk stearic acid predicted by mid-infrared spectra; C18:1 cis-9 = milk oleic acid predicted by mid-infrared spectra; SCFA = milk short-chain fatty acids predicted by mid-infrared spectra; MCFA = milk medium-chain fatty acids predicted by mid-infrared spectra; LCFA = milk long-chain fatty acids predicted by mid-infrared spectra; FP = milk fat percentage predicted by mid-infrared spectra; PP = milk protein percentage predicted by mid-infrared spectra; MY = milk yield.

[2] na = not applicable because trait has no units.

[3] NA = not applicable because data were not available.

	LPNEB	LEDS	LB_BHBA	NEFA	LIGF_1	GLU	LM_BHBA	CIT	LACE	C10:0	C14:0	C16:0	C18:0	C18:1 cis-9	SCFA	MCFA	LCFA	FP	PP	MY
LRNEB (Dataset I)	0.60	0.52	0.32	0.42	-0.24	-0.26	0.08	0.26	0.36	-0.11	-0.13	-0.03	0.41	0.48	0.11	-0.07	0.49	0.27	-0.12	0.01
LPNEB (Dataset I)	NA	0.75	0.47	0.64	-0.34	-0.39	0.09	0.36	0.54	-0.20	-0.26	-0.12	0.59	0.70	0.12	-0.18	0.71	0.33	-0.19	-0.07
LPNEB (Dataset II)	NA	0.80	0.47	0.79	-0.58	-0.54	0.36	0.36	0.62	-0.44	-0.36	-0.06	0.63	0.76	-0.09	-0.18	0.72	0.40	-0.17	0.20

Figure 2. Comparison of Pearson correlations observed for LRNEB and LPNEB with the 19 other traits in dataset I (n = 965) and for LPNEB with the 19 other traits in dataset II (n = 30,634). LRNEB = logarithm measured probability NEB; LPNEB = logarithm probability NEB predicted by mid-infrared spectra; LEDS = logarithm probability EDS; LB_BHBA = $\log_{10}$ blood β-hydroxybutyric acid predicted by mid-infrared spectra; NEFA = blood nonesterified fatty acids predicted by mid-infrared spectra; LIGF-1 = $\log_{10}$ blood IGF-1 predicted by mid-infrared spectra; GLU = blood glucose predicted by mid-infrared spectra; LM_BHBA = $\log_{10}$ milk β-hydroxybutyric acid predicted by mid-infrared spectra; CIT = milk citrate predicted by mid-infrared spectra; LACE = $\log_{10}$ milk acetone predicted by mid-infrared spectra; C10:0 = milk decanoic acid predicted by mid-infrared spectra; C14:0 = milk myristic acid predicted by mid-infrared spectra; C16:0 = milk palmitic acid predicted by mid-infrared spectra; C18:0 = milk stearic acid predicted by mid-infrared spectra; C18:1 *cis*-9 = milk oleic acid predicted by mid-infrared spectra; SCFA = milk short-chain fatty acids predicted by mid-infrared spectra; MCFA = milk medium-chain fatty acids predicted by mid-infrared spectra; LCFA = milk long-chain fatty acids predicted by mid-infrared spectra; FP = milk fat percentage predicted by mid-infrared spectra; PP = milk protein percentage predicted by mid-infrared spectra; MY = milk yield; NA = not applicable because data not available.

off-diagonals at convergence, as presented by Misztal et al. (1995), were available to check the efficiency of the multiple-diagonalization algorithm. Perfect multiple-diagonalization will result in zero off-diagonal elements. In this study, the values of 0.42×10^{-3} for the permanent environment and 0.11×10^{-3} for genetic (co)variances indicate excellent diagonalization. This low relative off-diagonal elements demonstrate that the optimization process had effectively converged leading to correct estimations of variances and covariances partitioning variance components.

Heritability, Genetic, and Phenotypic Correlations. For each trait (including LPNEB, LEDS, 15 biomarkers, and 3 production traits), the h^2 was calculated using the following equation:

$$h^2 = \frac{\sigma_a^2}{\sigma_a^2 + \sigma_p^2 + \sigma_e^2},$$

where σ_a^2, σ_p^2, and σ_e^2 represent the additive genetic, permanent environmental, and residual variance, respectively.

Genetic and phenotypic correlations were computed based on the estimated (co)variance components with genetic correlations being defined as the ratio of genetic covariances to the square root of the product of the corresponding variances and, similarly, phenotypic correlations being defined as the ratio of phenotypic covariances to the square root of the product of the corresponding variances. The required phenotypic covariance and variance are obtained by summing the relevant covariance components.

Because the MTC program used EM-REML, no SE were directly available. At convergence, the approxi-

mate SE of all estimated parameters were determined using the algorithm by Meyer and Houle (2013), as implemented in the BLUPF90+ software (version 2.48; https://nce.ads.uga.edu/html/projects/programs/), through the computation of the average information matrix.

Quantifying the Ability of the 19 Other Traits to Genetically Predict LPNEB

The abilities of the other traits to predict genetically LPNEB were investigated using selection index theory (Van Vleck, 1993), by partitioning the genetic variance for LPNEB into contributions from the other 19 traits. This was done using the estimated genetic correlation matrix for dataset II representing standardized covariances. The partitioning process was conducted as follows for each trait or set of traits (i.e., LEDS and the other 18 traits):

1. Standardized genetic covariances (i.e., correlations) between LPNEB and the identified trait(s) were extracted and organized into a vector **c**;
2. Standardized genetic covariances among the identified traits were extracted and compiled into a matrix **G**;
3. A vector of regression coefficients **b** was obtained as $(\mathbf{c'G^{-1}})'$;
4. Explained variance was computed as $\mathbf{b'Gb} = \mathbf{c'G^{-1}GG^{-1}c} = \mathbf{c'G^{-1}c}$;
5. Finally, the genetic variance was partitioned into explained and unexplained components by comparing the explained variance to the total variance (assumed here to be equal to 1).
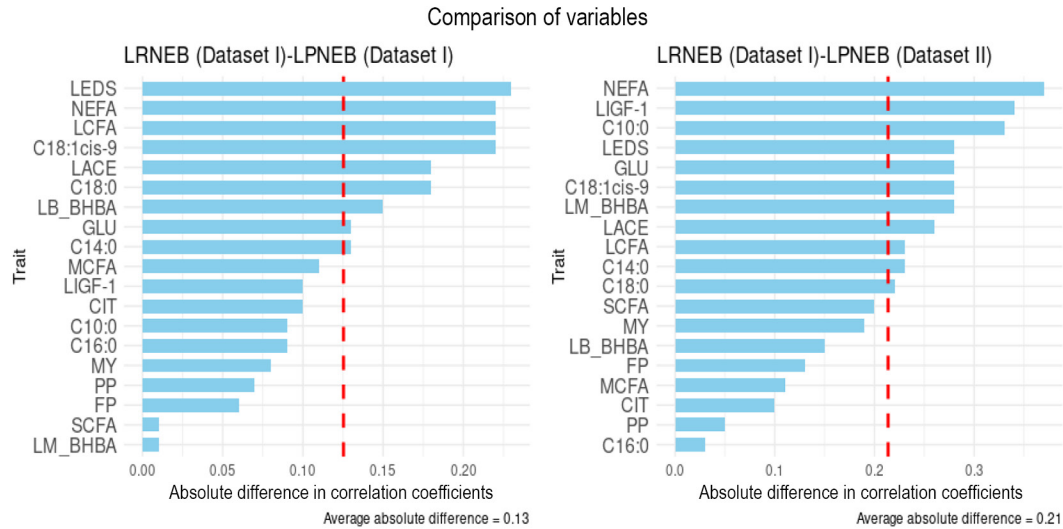
Figure 3. Absolute differences between Pearson correlations comparing LRNEB (dataset I) with LPNEB from datasets I and II for the other 19 traits. LEDS = logarithm probability EDS; LB_BHBA = log_{10} blood β-hydroxybutyric acid predicted by mid-infrared spectra; NEFA = blood nonesterified fatty acids predicted by mid-infrared spectra; LIGF-1 = log_{10} blood IGF-1 predicted by mid-infrared spectra; GLU = blood glucose predicted by mid-infrared spectra; LM_BHBA = log_{10} milk beta-hydroxybutyric acid predicted by mid-infrared spectra; CIT = milk citrate predicted by mid-infrared spectra; LACE = log_{10} milk acetone predicted by mid-infrared spectra; C10:0 = milk decanoic acid predicted by mid-infrared spectra; C14:0 = milk myristic acid predicted by mid-infrared spectra; C16:0 = milk palmitic acid predicted by mid-infrared spectra; C18:0 = milk stearic acid predicted by mid-infrared spectra; C18:1 *cis*-9 = milk oleic acid predicted by mid-infrared spectra; SCFA = milk short-chain fatty acids predicted by mid-infrared spectra; MCFA = milk medium-chain fatty acids predicted by mid-infrared spectra; LCFA = milk long-chain fatty acids predicted by mid-infrared spectra; FP = milk fat percentage predicted by mid-infrared spectra; PP = milk protein percentage predicted by mid-infrared spectra; MY = milk yield.

Causal Effects of Predicted EB on the Other 19 Traits

The (co)variance components estimated from the multitrait model can be transformed posteriorly into the (co)variance decomposition of a recursive model (Varona and González-Recio, 2023) to detect the causal effects. During this transformation process, the structural coefficients of LPNEB for the remaining 19 traits were computed. Furthermore, we assessed the causal effect of LPNEB on these 19 traits by analyzing the percentage change in genetic (or phenotypic) variance between the multitrait model and the recursive model. Additional data preparation and processing were done using R (version 4.2.1, https://www.r-project.org/).
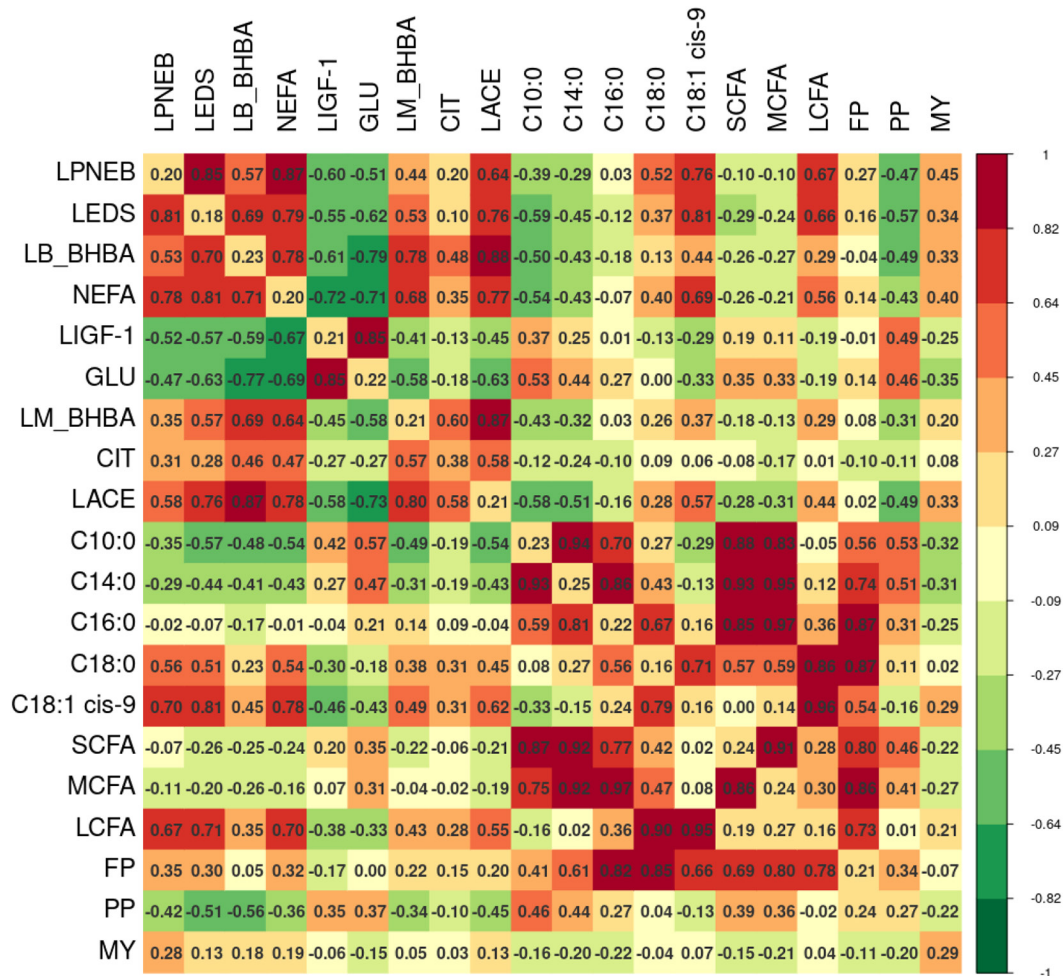
RESULTS AND DISCUSSION

Descriptive Statistics

The descriptive statistics of LRNEB, LPNEB, LEDS, 15 biomarkers, and 3 production traits for the 2 datasets from first-parity cows are presented in Table 2. The predicted values for all traits used in this study were within the range of the measured data used previously for the initial calibration (i.e., model developments) of the MIR prediction models for traits. In dataset I, it needs to be noted that mean raw data for EB showed values of −3.11 Mcal/d for measured EB and −3.05 for predicted EB with SD of 6.26 and 4.35, respectively. In dataset II the mean was 0.01 for predicted EB with an SD of 3.70, highlighting the differences between the 2 datasets. As explained earlier, comparison of descriptive parameters of LRNEB, LPNEB, LEDS across traits and datasets should be considered with great caution. The averages of 4 predicted blood traits LB_BHBA, NEFA, LIGF-1, and GLU in dataset II were similar to those found in dataset I. The average predicted B_BHBA, NEFA, and GLU in dataset II were consistent with the measured data of these traits from other studies (Kostensalo et al., 2023; Mota et al., 2023).

The mean values of predicted 11 milk biomarkers and PP in both datasets were similar, and these values were in line with previous studies (Soyeurt et al., 2006, 2011; Grelet et al., 2016, 2024). The datasets used in the current study are completely independent from those cited in the referenced studies. The mean MY, after correction for parity, were similar between the 2 datasets in this study, which is also consistent with the findings in the larger dataset that Atashi et al. (2024) used representing the Walloon dairy cattle population. The value for FP in dataset I was higher (4.00%) compared with dataset II (3.79%). This fact and the differences in EB described previously could indicate differences between datasets in energy intake and fiber in the diet.

	LPNEB	LEDS	LB_BHBA	NEFA	LIGF-1	GLU	LM_BHBA	CIT	LACE	C10:0	C14:0	C16:0	C18:0	C18:1 cis-9	SCFA	MCFA	LCFA	FP	PP	MY
LPNEB	0.20	0.85	0.57	0.87	-0.60	-0.51	0.44	0.20	0.64	-0.39	-0.29	0.03	0.52	0.76	-0.10	-0.10	0.67	0.27	-0.47	0.45
LEDS	0.81	0.18	0.69	0.79	-0.55	-0.62	0.53	0.10	0.76	-0.59	-0.45	-0.12	0.37	0.81	-0.29	-0.24	0.66	0.16	-0.57	0.34
LB_BHBA	0.53	0.70	0.23	0.78	-0.61	-0.79	0.78	0.48	0.88	-0.50	-0.43	-0.18	0.13	0.44	-0.26	-0.27	0.29	-0.04	-0.49	0.33
NEFA	0.78	0.81	0.71	0.20	-0.72	-0.71	0.68	0.35	0.77	-0.54	-0.43	-0.07	0.40	0.69	-0.26	-0.21	0.56	0.14	-0.43	0.40
LIGF-1	-0.52	-0.57	-0.59	-0.67	0.21	0.85	-0.41	-0.13	-0.45	0.37	0.25	0.01	-0.13	-0.29	0.19	0.11	-0.19	-0.01	0.49	-0.25
GLU	-0.47	-0.63	-0.77	-0.69	0.85	0.22	-0.58	-0.18	-0.63	0.53	0.44	0.27	0.00	-0.33	0.35	0.33	-0.19	0.14	0.46	-0.35
LM_BHBA	0.35	0.57	0.69	0.64	-0.45	-0.58	0.21	0.60	0.67	-0.43	-0.32	0.03	0.26	0.37	-0.18	-0.13	0.29	0.08	-0.31	0.20
CIT	0.31	0.28	0.46	0.47	-0.27	-0.27	0.57	0.38	0.58	-0.12	-0.24	-0.10	0.09	0.06	-0.08	-0.17	0.01	-0.10	-0.11	0.08
LACE	0.58	0.76	0.82	0.78	-0.58	-0.73	0.80	0.58	0.21	-0.58	-0.51	-0.16	0.28	0.57	-0.28	-0.31	0.44	0.02	-0.49	0.33
C10:0	-0.35	-0.57	-0.48	-0.54	0.42	0.57	-0.49	-0.19	-0.54	0.23	0.94	0.70	0.27	-0.29	0.88	0.63	-0.05	0.56	0.53	-0.32
C14:0	-0.29	-0.44	-0.41	-0.43	0.27	0.47	-0.31	-0.19	-0.43	0.92	0.25	0.86	0.43	-0.13	0.93	0.95	0.12	0.74	0.51	-0.31
C16:0	-0.02	-0.07	-0.17	-0.01	-0.04	0.21	0.14	0.09	-0.04	0.59	0.81	0.22	0.67	0.16	0.85	0.87	0.36	0.87	0.31	-0.25
C18:0	0.56	0.51	0.23	0.54	-0.30	-0.18	0.38	0.31	0.45	0.08	0.27	0.56	0.16	0.71	0.57	0.59	0.86	0.87	0.11	0.02
C18:1 cis-9	0.70	0.81	0.45	0.78	-0.46	-0.43	0.49	0.31	0.62	-0.33	-0.15	0.24	0.79	0.16	0.00	0.14	0.96	0.54	-0.16	0.29
SCFA	-0.07	-0.26	-0.25	-0.24	0.20	0.35	-0.22	-0.06	-0.21	0.87	0.82	0.77	0.42	0.02	0.24	0.91	0.28	0.80	0.46	-0.22
MCFA	-0.11	-0.20	-0.26	-0.16	0.07	0.31	-0.04	-0.02	-0.19	0.75	0.92	0.97	0.47	0.08	0.88	0.24	0.30	0.85	0.41	-0.27
LCFA	0.67	0.71	0.35	0.70	-0.38	-0.33	0.43	0.28	0.55	-0.16	0.02	0.36	0.90	0.95	0.19	0.27	0.16	0.73	0.01	0.21
FP	0.35	0.30	0.05	0.32	-0.17	0.00	0.22	0.15	0.20	0.41	0.61	0.82	0.85	0.66	0.69	0.80	0.78	0.21	0.34	-0.07
PP	-0.42	-0.51	-0.56	-0.36	0.35	0.37	-0.34	-0.10	-0.45	0.46	0.44	0.27	0.04	-0.13	0.39	0.36	-0.02	0.24	0.27	-0.22
MY	0.28	0.13	0.18	0.19	-0.06	-0.15	0.05	0.03	0.13	-0.16	-0.20	-0.22	-0.04	0.07	-0.15	-0.21	0.04	-0.11	-0.20	0.29

Figure 4. The h^2 (diagonal) of 20 traits and their genetic (above diagonal), and phenotypic (below diagonal) correlations. The ranges of SE for h^2, genetic correlation, and phenotypic correlation are from 0.01 to 0.02, 0.01 to 0.07, and below 0.01 to 0.06, respectively. LPNEB = logarithm probability NEB predicted by mid-infrared spectra; LEDS = logarithm probability EDS; LB_BHBA = $\log_{10}$ blood β-hydroxybutyric acid predicted by mid-infrared spectra; NEFA = blood nonesterified fatty acids predicted by mid-infrared spectra; LIGF-1 = $\log_{10}$ blood IGF-1 predicted by mid-infrared spectra; GLU = blood glucose predicted by mid-infrared spectra; LM_BHBA = $\log_{10}$ milk β-hydroxybutyric acid predicted by mid-infrared spectra; CIT = milk citrate predicted by mid-infrared spectra; LACE = $\log_{10}$ milk acetone predicted by mid-infrared spectra; C10:0 = milk decanoic acid predicted by mid-infrared spectra; C14:0 = milk myristic acid predicted by mid-infrared spectra; C16:0 = milk palmitic acid predicted by mid-infrared spectra; C18:0 = milk stearic acid predicted by mid-infrared spectra; C18:1 *cis*-9 = milk oleic acid predicted by mid-infrared spectra; SCFA = milk short-chain fatty acids predicted by mid-infrared spectra; MCFA = milk medium-chain fatty acids predicted by mid-infrared spectra; LCFA = milk long-chain fatty acids predicted by mid-infrared spectra; FP = milk fat percentage predicted by mid-infrared spectra; PP = milk protein percentage predicted by mid-infrared spectra; MY = milk yield.

Pearson Correlation of Measured EB, Predicted EB with Other 19 Traits

The r between LRNEB (only present in dataset I) and LPNEB with the other 19 traits in datasets I and II are shown in Figure 2 and Supplemental Table S1 (see Notes). Relevant *P*-values can be found in Supplemental Table S2 (see Notes).

The r coefficient computed between LRNEB and LPNEB in dataset I was 0.60, reflecting the coefficient of determination of cross-validation ($\mathbf{R^2cv}$) known from the calibration process (Table 1). This indicates a mod-

erate but significant relationship between LRNEB and LPNEB. In the same dataset I, the r calculated between LRNEB and LEDS was 0.52, suggesting a comparatively slightly weaker association between LRNEB and LEDS. This finding aligns with expectations, because the predictive equation for EDS was not directly derived from EB, in contrast to prediction of EB. The absolute differences in r between LRNEB and the other traits with the corresponding values between LPNEB and the other traits are given in Figure 3. This low value of 0.13 suggests that despite moderate correlations between LRNEB and LPNEB these 2 traits showed a similar relationship

Table 3. Structural coefficients and causal effects (phenotypic and genetic variances changed percentage) of $\log_{10}$ predicted NEB (LPNEB) on the 19 traits[1]

Trait	Structural coefficients	Phenotypic variance change (%)	Genetic variance change (%)
LEDS	−0.44	73.66	71.51
In blood			
LB_BHBA	−0.36	38.89	30.88
NEFA	−6.86	81.06	75.43
LIGF-1	0.37	46.25	33.22
GLU	0.60	35.32	17.29
In milk			
LM_BHBA	−0.23	25.51	18.30
CIT	−1.57	7.75	4.18
LACE	−0.50	47.19	39.79
C10:0	0.05	19.82	12.55
C14:0	0.15	15.58	5.32
C16:0	0.17	−0.20	−5.98
C18:0	−0.07	14.98	18.97
C18:1 *cis*-9	−0.42	62.37	54.83
SCFA	0.07	3.54	−3.85
MCFA	0.41	4.45	−3.94
LCFA	−0.53	42.26	40.14
FP	−0.03	0.41	0.73
PP	0.70	36.90	22.88
MY	−2.38	40.59	−31.53

[1]LEDS = logarithm probability EDS; LB_BHBA = $\log_{10}$ blood β-hydroxybutyric acid predicted by mid-infrared spectra; NEFA = blood nonesterified fatty acids predicted by mid-infrared spectra; LIGF-1 = $\log_{10}$ blood IGF-1 predicted by mid-infrared spectra; GLU = blood glucose predicted by mid-infrared spectra; LM_BHBA = $\log_{10}$ milk β-hydroxybutyric acid predicted by mid-infrared spectra; CIT = milk citrate predicted by mid-infrared spectra; LACE = $\log_{10}$ milk acetone predicted by mid-infrared spectra; C10:0 = milk decanoic acid predicted by mid-infrared spectra; C14:0 = milk myristic acid predicted by mid-infrared spectra; C16:0 = milk palmitic acid predicted by mid-infrared spectra; C18:0 = milk stearic acid predicted by mid-infrared spectra; C18:1 *cis*-9 = milk oleic acid predicted by mid-infrared spectra; SCFA = milk short-chain fatty acids predicted by mid-infrared spectra; MCFA = milk medium-chain fatty acids predicted by mid-infrared spectra; LCFA = milk long-chain fatty acids predicted by mid-infrared spectra; FP = milk fat percentage predicted by mid-infrared spectra; PP = milk protein percentage predicted by mid-infrared spectra; MY = milk yield.

with the other studied traits, indicating that despite working with MIR-predicted traits some conclusions that are also valid for LRNEB can be drawn. This preliminary hypothesis was confirmed by comparing r for LRNEB (dataset I) and LPNEB (dataset II), which were similar to the values reported previously and showed a mean absolute difference of 0.21.

When compared to the literature, our results in dataset I for LRNEB with blood NEFA (0.42) were in line with, but slightly lower than, those reported by Pires et al. (2022) for directly measured NEFA and EB. Our results indicated that fatty acids C18:1 *cis*-9 (0.48) and C18:0 (0.41) showed a strong r with LRNEB compared with the other milk biomarkers examined. These findings align with the results reported by Churakov et al. (2021), which also indicated that C18:1 *cis*-9 and C18:0 were correlated with NEB. The r calculated between LCFA and LRNEB was 0.49, which is in line with literature (e.g., Guinguina et al., 2021).

Genetic Parameters

At convergence, relative off-diagonals were 0.42×10^{-3} for permanent environment and 0.11×10^{-3} for ge-

netic (co)variances, showing an excellent level of diagonalization. Figure 4 shows the h^2 (diagonal), genetic correlations (above diagonal), and phenotypic correlations (below diagonal) of the 20 traits examined (LPNEB, LEDS, 15 biomarkers, and 3 production traits) estimated by a 20-trait repeatability model. All the studied traits (n = 20) had a moderate h^2 (range: 0.16–0.29) and an SE ranging from 0.01 to 0.02, except for CIT which had a higher h^2 (0.38) with an SE of 0.02 (Supplemental Table S3, see Notes). All h^2 were significantly different from zero (Supplemental Table S4, see Notes) The h^2 of LPNEB was similar to those reported in previous studies with directly measured EB (McParland et al., 2015; Becker et al., 2021). Becker et al. (2021) showed that the h^2 of measured EB was not stable during lactation, ranging from 0.15 to 0.31. The h^2 of 4 examined predicted blood biomarkers (LB_BHBA, NEFA, LIGF-1, and GLU) agreed with those reported by van der Drift et al. (2012), Benedet et al. (2020), and Hayhurst et al. (2009). However, Hayhurst et al. (2009) showed that the h^2 of IGF-1 varied in different populations, ranging from 0.21 to 0.66. The h^2 of LM_BHBA, CIT, and LACE were similar to those reported with a larger dataset (Ranaraja et al., 2018; Chen et al., 2024). The h^2 of the other 8
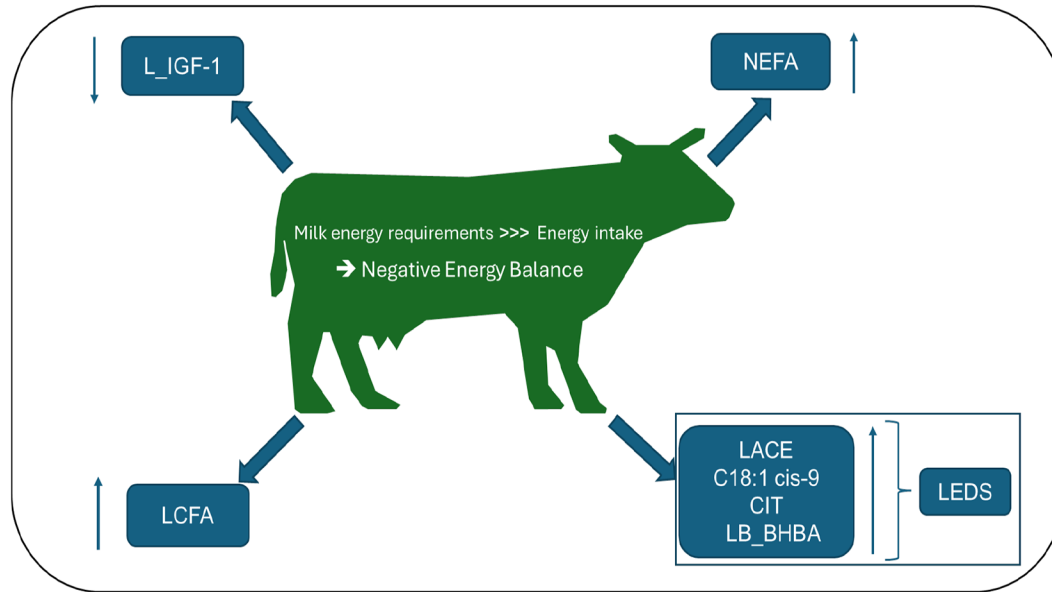
Figure 5. Reaction of 7 important biomarkers as reported in this study when cows had NEB in early lactation (LIGF-1 = $\log_{10}$ blood IGF-1 predicted by mid-infrared spectra; NEFA = blood nonesterified fatty acids predicted by mid-infrared spectra; LCFA = milk long-chain fatty acids predicted by mid-infrared spectra; LACE = $\log_{10}$ milk acetone predicted by mid-infrared spectra; C18:1 *cis*-9 = milk oleic acid predicted by mid-infrared spectra; CIT = milk citrate predicted by mid-infrared spectra; LB_BHBA = $\log_{10}$ blood β-hydroxybutyric acid predicted by mid-infrared spectra; LEDS = logarithm probability EDS). The arrows represent the direction of change in trait values when dairy cows are in NEB. The upward arrow indicates an increase in the trait value, and the downward arrow indicates a decrease in the trait value.

milk biomarkers and 3 production traits were within the range estimated by random regression models (Bastin et al., 2011; Paiva et al., 2022).

The absolute genetic correlation between LPNEB and 9 out of the remaining 19 traits (LEDS, LB_BHBA, NEFA, LIGF-1, GLU, LACE, C18:0, C18:1 *cis*-9, and LCFA) were higher than 0.50, and LPNEB has the highest genetic correlation with NEFA (0.87). In early lactation, blood NEFA has been considered by previous studies to be the best single biomarker of NEB (Oikonomou et al., 2008; Andjelić et al., 2022).

As was mentioned previously (Franceschini et al., 2022), EDS included EB, which explains the high correlation of 0.85 with LPNEB. Moreover, EDS included also C18:1 *cis*-9, so it showed the second-highest genetic correlation (0.81). The third-highest genetic correlation was found between LPNEB and C18:1 *cis*-9 (0.76). Recently, Churakov et al. (2021) and Guinguina et al. (2021) reported that the oleic acid is a good biomarker for identifying the NEB state in dairy cows. We also found that the genetic correlation values between LPNEB and PP and MY were −0.47 and 0.45, respectively. The range of genetic correlation between the direct EB and energy-corrected MY and PP in early lactation (15–45 DIM) reported in the literature were −0.57 to −0.39 and 0.30 to 0.53, respectively (Buttchereit et al., 2011).

The genetic correlation values among the other 18 traits were also within a reasonable ranges. For example,

the genetic correlation estimated among NEFA and LM_BHBA, LACE, and C18:1 *cis*-9 were similar to that reported by Mehtiö et al. (2020). The 8 examined fatty acids (**FA**) had high genetic correlation with FP (>0.50), which was similar to results reported by Bastin et al. (2011).

The phenotypic correlations estimated between each pair of the 20 traits were generally similar to the corresponding genetic correlations, with the phenotypic correlations being slightly lower than the genetic correlations. The average absolute difference of genetic correlations and phenotypic correlations for LPNEB with the other 19 traits was 0.06, with a minimum of 0.00 for C14:0, LCFA and a maximum of 0.17 for MY. The average absolute difference of genetic correlations and phenotypic correlations for LEDS with the other 19 traits was 0.06, with a minimum of 0.00 for LACE, C18:1*cis*-9 and a maximum of 0.21 for MY.

The absolute phenotypic correlations between LPNEB and 8 traits (LEDS, LB_BHBA, NEFA, LIGF-1, LACE, C18:0, C18:1 *cis*-9, and LCFA) were higher than 0.50, and the phenotypic correlation of LEDS was the highest (0.81). The phenotypic correlations between LPNEB and NEFA, C18:1 *cis*-9 were 0.78 and 0.70, respectively. The high phenotypic correlations of these 3 traits were consistent with the genetic correlations mentioned previously. A severe NEB state in cattle expressed by high LPNEB will increase 7 of the 8 traits (LEDS, LB_BHBA,

NEFA, LACE, C18:0, C18:1 *cis*-9, LCFA) and decrease 1 biomarker (LIGF-1).

Quantifying the Ability of the 19 Other Traits to Genetically Predict LPNEB

The quantification of the ability of the other 19 traits to predict genetically LPNEB, expressed as the fraction of the genetic variance of LPNEB that could be predicted by other traits, was computed to be 65% for LEDS alone, 62% for NEFA alone, 82% for all 15 biomarkers alone, 85% for all other 18 traits, excluding LEDS, and 89% combining LEDS and the other traits. These results seem to indicate that LEDS contains additional information useful for predicting LPNEB and not contained in the other 18 traits. This result could be due to the specific approach (i.e., cluster analysis) used by Franceschini et al. (2022), leading to the definition of a specific NEB-related cluster (i.e., his cluster 4), which is the basis of EDS, and respectively LEDS, as used in this study.

Causal Effects of Predicted EB on the Other 19 Traits

The structural coefficients and causal effects (phenotypic and genetic variances changed percentage) of the LPNEB on the other 19 traits are shown in Table 3. Structural coefficients represent the amount of change in trait *i* with one unit change of LPNEB expressed as decrease in trait *i* (i.e., which is equivalent to expressing trait *i* but keeping LPNEB constant). Positive values for structural coefficients for NEFA, CIT, and MY mean that higher values of LPNEB lead to higher values for these traits. However, it is well known that the NEB state of cattle is caused by insufficient energy intake to produce MY, and therefore the causality of MY and the NEB state might be reversed (i.e., changes in MY lead to higher NEB) even if the fact that animals are in a state of NEB leads to less MY. The NEFA can measure fat mobilization in cattle, which is an important indicator of the NEB state in cattle (Zachut et al., 2020). Citrate is implicated in this process and is an inhibitor of de novo FA synthesis in dairy cows (Garnsworthy et al., 2006). Citrate is also considered a potential early biomarker for assessing the NEB state in dairy cows (Bjerre-Harpøth et al., 2012; Xu et al., 2020).

Table 3 also shows phenotypic and genetic variance changes due to fitting the recursiveness to LPNEB, with positive values indicating a decrease and negative values an increase. In total 8 traits (LEDS, LB_BHBA, NEFA, LIGF-1, LACE, C18:1 *cis*-9, LCFA and MY) were selected based on the results of phenotypic and genetic variance change (both absolute values higher than 30%). The top 3 of the 8 traits were NEFA, LEDS, C18:1 *cis*-9, which are the same as the genetic correlations. The phenotypic (positive) and genetic (negative) variance change of MY

were in different directions, which again supports the idea that MY and LPNEB had an inversed causality.

Based on our results (r, genetic and phenotypic correlations, explained variances, structural coefficients, and caused effects) we can suggest 8 out of the 19 examined traits (LEDS, LB_BHBA, NEFA, LIGF-1, CIT, LACE, C18:1 *cis*-9, LCFA) as being highly related to LPNEB. Our results indicated that the most relevant biomarker was NEFA, which is already well-recognized in literature (e.g., Macrae et al., 2019). However, NEFA is also one of MIR-based biomarkers based on the poorest calibrations (Table 1), therefore we want to express here some caution. The observed recursive relationships between 8 traits with LPNEB are summarized in Figure 5, indicating that high LPNEB will affect the other 7 individual biomarkers in the direction indicated by the arrows. Moreover, based on its definition, LEDS represents 4 (LB_BHBA, CIT, LACE, C18:1 *cis*-9) of the major single biomarkers considered affected by the NEB state.

CONCLUSIONS

This study explored the relationships among LRNEB, LPNEB, LEDS, 15 biomarkers, and 3 production traits. The LPNEB showed a strong genetic correlation with NEFA, confirming its relevance as a biomarker, despite its lower prediction accuracy. The genetic correlation patterns between LRNEB and LPNEB with other traits were similar, suggesting LPNEB can be cautiously used in place of LRNEB. The novel trait LEDS exhibited the strongest causal association with NEB and demonstrated a high genetic ability to predict LPNEB (65%), surpassing NEFA (62%). A recursive model identified strong causal links between predicted NEB and 8 traits, also strengthening the case for using LEDS as an indicator of NEB. These findings enhance our understanding of the genetic, phenotypic, and causal relationships of NEB with the other 19 studied traits. Further research is needed to explore the genetic architecture of these traits and of their relationships

mental materials for this article are available at https://data.mendeley.com/datasets/gh9pwf8fph/2. Author contributions are as follows: Hongqing Hu, funding acquisition, formal analysis, and writing (original draft); Sébastien Franceschini, data curation and writing (review and editing); Pauline Lemal, validation and writing (review and editing); Clément Grelet, data curation and writing (review and editing); Yansen Chen, data curation and writing (review and editing); Hadi Atashi, validation and writing (review and editing); Katrien Wijnrocx, validation and writing (review and editing); Hélène Soyeurt, validation and writing (review and editing); Nicolas Gengler, conceptualization, funding acquisition, methodology, project administration, software, supervision, validation, and writing (review and editing). No human or animal subjects were used, so this analysis did not require approval by an Institutional Animal Care and Use Committee or Institutional Review Board. The authors have not stated any conflicts of interest.

Nonstandard abbreviations used: ACE = milk acetone predicted by mid-infrared spectra; B_BHBA = blood β-hydroxybutyric acid predicted by mid-infrared spectra; BHBA = β-hydroxybutyrate acid; C10:0 = milk decanoic fatty acid predicted by mid-infrared spectra; C14:0 = milk myristic fatty acid predicted by mid-infrared spectra; C16:0 = milk palmitic fatty acid predicted by mid-infrared spectra; C18:0 = milk stearic fatty acid predicted by mid-infrared spectra; C18:1 cis-9 = milk oleic fatty acid predicted by mid-infrared spectra; CIT = milk citrate predicted by mid-infrared spectra; EB = energy balance; EDS = energy deficit score; EM-REML = expectation maximization REML; FA = fatty acid; FP = milk fat percentage predicted by mid-infrared spectra; GLU = blood glucose predicted by mid-infrared spectra; LACE = $\log_{10}$ milk acetone predicted by mid-infrared spectra; LB_BHBA = $\log_{10}$ blood β-hydroxybutyric acid predicted by mid-infrared spectra; LCFA = milk long-chain fatty acids predicted by mid-infrared spectra; LEDS = logarithm probability energy deficit score; LIGF-1 = $\log_{10}$ blood insulin-like growth factor 1 predicted by mid-infrared spectra; LM_BHBA = $\log_{10}$ milk β-hydroxybutyric acid predicted by mid-infrared spectra; LPNEB = logarithm probability negative energy balance predicted by mid-infrared spectra; LRNEB = logarithm measured probability negative energy balance; M_BHBA = milk β-hydroxybutyric acid predicted by mid-infrared spectra; MCFA = milk medium-chain fatty acids predicted by mid-infrared spectra; MIR = mid-infrared; MY = milk yield; NA = not applicable because data were not available; na = not applicable because trait has no units; NEB = negative energy balance; NEFA = blood nonesterified fatty acids predicted by mid-infrared spectra; PEB = energy balance predicted by mid-infrared spectra; PNEB = negative energy balance predicted by mid-infrared spectra; PP = milk protein percentage predicted by mid-infrared spectra; R^2cv = coefficient of determination of cross-validation; REB = measured energy balance; RNEB = measured negative energy balance; RMSEcv = root mean square error of cross-validation; SCFA = milk short-chain fatty acids predicted by mid-infrared spectra.

REFERENCES

Andjelić, B., R. Djoković, M. Cincović, S. Bogosavljević-Bošković, M. Petrović, J. Mladenović, and A. Čukić. 2022. Relationships between milk and blood biochemical parameters and metabolic status in dairy cows during lactation. Metabolites 12:733. https://doi.org/10.3390/metabo12080733.

Atashi, H., Y. Chen, S. Vanderick, X. Hubin, and N. Gengler. 2024. Single-step genome-wide association analyses for milk urea concentration in Walloon Holstein cows. J. Dairy Sci. 107:3020–3031. https://doi.org/10.3168/jds.2023-23902.

Bastin, C., N. Gengler, and H. Soyeurt. 2011. Phenotypic and genetic variability of production traits and milk fatty acid contents across days in milk for Walloon Holstein first-parity cows. J. Dairy Sci. 94:4152–4163. https://doi.org/10.3168/jds.2010-4108.

Baumgard, L. H., L. J. Odens, J. K. Kay, R. P. Rhoads, M. J. VanBaale, and R. J. Collier. 2006. Does negative energy balance (NEBAL) limit milk synthesis in early lactation? Pages 181–187 in Proc. Southwest Nutr. Conf. Accessed Feb. 22, 2025. https://rapp.ualberta.ca/wp-content/uploads/sites/57/wcds_archive/Archive/2007/Manuscripts/Lance.pdf. https://rapp.ualberta.ca/wpcontent/uploads/sites/57/wcds_archive/Archive/2007/Manuscripts/Lance.pdf.

Becker, V. A. E., E. Stamer, H. Spiekers, and G. Thaller. 2021. Residual energy intake, energy balance, and liability to diseases: Genetic parameters and relationships in German Holstein dairy cows. J. Dairy Sci. 104:10970–10978. https://doi.org/10.3168/jds.2021-20382.

Benedet, A., A. Costa, M. De Marchi, and M. Penasa. 2020. Heritability estimates of predicted blood β-hydroxybutyrate and nonesterified fatty acids and relationships with milk traits in early-lactation Holstein cows. J. Dairy Sci. 103:6354–6363. https://doi.org/10.3168/jds.2019-17916.

Berry, D. P., B. Horan, M. O'Donovan, F. Buckley, E. Kennedy, M. McEvoy, and P. Dillon. 2007. Genetics of grass dry matter intake, energy balance, and digestibility in grazing Irish dairy cows. J. Dairy Sci. 90:4835–4845. https://doi.org/10.3168/jds.2007-0116.

Bjerre-Harpøth, V., N. C. Friggens, V. M. Thorup, T. Larsen, B. M. Damgaard, K. L. Ingvartsen, and K. M. Moyes. 2012. Metabolic and production profiles of dairy cows in response to decreased nutrient density to increase physiological imbalance at different stages of lactation. J. Dairy Sci. 95:2362–2380. https://doi.org/10.3168/jds.2011-4419.

Buttchereit, N., E. Stamer, W. Junge, and G. Thaller. 2011. *Short communication:* Genetic relationships among daily energy balance, feed intake, body condition score, and fat to protein ratio of milk in dairy cows. J. Dairy Sci. 94:1586–1591. https://doi.org/10.3168/jds.2010-3396.

Chen, Y., H. Hu, H. Atashi, C. Grelet, K. Wijnrocx, P. Lemal, and N. Gengler. 2024. Genetic analysis of milk citrate predicted by milk mid-infrared spectra of Holstein cows in early lactation. J. Dairy Sci. 107:3047–3061. https://doi.org/10.3168/jds.2023-23903.

Chen, Y., S. Vanderick, R. R. Mota, C. GreletGplusE Consortium, and N. Gengler. 2021. Estimation of genetic parameters for predicted nitrogen use efficiency and losses in early lactation of Holstein cows. J. Dairy Sci. 104:4413–4423. https://doi.org/10.3168/jds.2020-18849.

Churakov, M., J. Karlsson, A. Edvardsson Rasmussen, and K. Holtenius. 2021. Milk fatty acids as indicators of negative energy balance of dairy cows in early lactation. Animal 15:100253. https://doi.org/10.1016/j.animal.2021.100253.

Collard, B. L., P. J. Boettcher, J. C. M. Dekkers, D. Petitclerc, and L. R. Schaeffer. 2000. Relationships between energy balance and health

traits of dairy cattle in early lactation. J. Dairy Sci. 83:2683–2690. https://doi.org/10.3168/jds.S0022-0302(00)75162-9.

Franceschini, S., C. Grelet, J. Leblois, N. Gengler, and H. Soyeurt. GplusE Consortium. 2022. Can unsupervised learning methods applied to milk recording big data provide new insights into dairy cow health? J. Dairy Sci. 105:6760–6772. https://doi.org/10.3168/jds.2022-21975.

Garnsworthy, P. C., L. L. Masson, A. L. Lock, and T. T. Mottram. 2006. Variation of milk citrate with stage of lactation and de novo fatty acid synthesis in dairy cows. J. Dairy Sci. 89:1604–1612. https://doi.org/10.3168/jds.S0022-0302(06)72227-5.

Grelet, C., C. Bastin, M. Gelé, J. B. Davière, M. Johan, A. Werner, R. Reding, J. A. Fernandez Pierna, F. G. Colinet, P. Dardenne, N. Gengler, H. Soyeurt, and F. Dehareng. 2016. Development of Fourier transform mid-infrared calibrations to predict acetone, β-hydroxybutyrate, and citrate contents in bovine milk through a European dairy network. J. Dairy Sci. 99:4816–4825. https://doi.org/10.3168/jds.2015-10477.

Grelet, C., P. Dardenne, H. Soyeurt, J. A. Fernandez, A. Vanlierde, F. Stevens, N. Gengler, and F. Dehareng. 2021. Large-scale phenotyping in dairy sector using milk MIR spectra: Key factors affecting the quality of predictions. Methods 186:97–111. https://doi.org/10.1016/j.ymeth.2020.07.012.

Grelet, C., J. A. Fernández Pierna, P. Dardenne, V. Baeten, and F. Dehareng. 2015. Standardization of milk mid-infrared spectra from a European dairy network. J. Dairy Sci. 98:2150–2160. https://doi.org/10.3168/jds.2014-8764.

Grelet, C., E. Froidmont, L. Foldager, M. Salavati, M. Hostens, C. P. Ferris, K. L. Ingvartsen, M. A. Crowe, M. T. Sorensen, J. A. Fernandez Pierna, A. Vanlierde, N. GenglerGplusE Consortium, and F. Dehareng. 2020. Potential of milk mid-infrared spectra to predict nitrogen use efficiency of individual dairy cows in early lactation. J. Dairy Sci. 103:4435–4445. https://doi.org/10.3168/jds.2019-17910.

Grelet, C., T. Larsen, M. A. Crowe, D. C. Wathes, C. P. Ferris, K. L. Ingvartsen, C. Marchitelli, F. Becker, A. Vanlierde, J. Leblois, U. Schuler, F. J. Auer, A. Köck, L. Dale, J. Sölkner, O. Christophe, J. Hummel, A. Mensching, J. A. Fernández Pierna, H. Soyeurt, M. Calmels, R. Reding, M. Gelé, Y. Chen, N. GenglerGplusE Consortium, and F. Dehareng. 2024. Prediction of key milk biomarkers in dairy cows through milk mid-infrared spectra and international collaborations. J. Dairy Sci. 107:1669–1684. https://doi.org/10.3168/jds.2023-23843.

Grelet, C., A. Vanlierde, F. Dehareng, E. Froidmont, and GplusE Consortium. 2017, Prediction of energy status of dairy cows using MIR milk spectra. Page 403 in Book of Abstracts of the 68th Annual Meeting of the European Federation of Animal Science, Tallin, Estonia. Wageningen Academic Publishers. https://hdl.handle.net/2268/224000.

Grelet, C., A. Vanlierde, M. Hostens, L. Foldager, M. Salavati, K. L. Ingvartsen, M. Crowe, M. T. Sorensen, E. Froidmont, C. P. Ferris, C. Marchitelli, F. Becker, T. Larsen, F. CarterGplusE Consortium, and F. Dehareng. 2019. Potential of milk mid-IR spectra to predict metabolic status of cows through blood components and an innovative clustering approach. Animal 13:649–658. https://doi.org/10.1017/S1751731118001751.

Guinguina, A., T. Yan, E. Trevisi, and P. Huhtanen. 2021. The use of an upgraded GreenFeed system and milk fatty acids to estimate energy balance in early-lactation cows. J. Dairy Sci. 104:6701–6714. https://doi.org/10.3168/jds.2020-19591.

Hayhurst, C., A. P. F. Flint, P. Løvendahl, J. A. Woolliams, and M. D. Royal. 2009. Genetic variation of metabolite and hormone concentration in UK Holstein-Friesian calves and the genetic relationship with economically important traits. J. Dairy Sci. 92:4001–4007. https://doi.org/10.3168/jds.2008-1130.

Ho, P. N., L. C. Marett, W. J. Wales, M. Axford, E. M. Oakes, and J. E. Pryce. 2020. Predicting milk fatty acids and energy balance of dairy cows in Australia using milk mid-infrared spectroscopy. Anim. Prod. Sci. 60:164–168. https://doi.org/10.1071/AN18532.

ICAR. 2022. Procedure 2 of Section 2 of ICAR Guidelines—Computing of Accumulated Lactation Yield. Accessed Dec. 29, 2023. https://www.icar.org/Guidelines/02-Procedure-2-Computing-Lactation-Yield.pdf.

Kostensalo, J., M. Lidauer, B. Aernouts, P. Mäntysaari, T. Kokkonen, P. Lidauer, and T. Mehtiö. 2023. Short communication: Predicting blood plasma non-esterified fatty acid and beta-hydroxybutyrate concentrations from cow milk—Addressing systematic issues in modelling. Animal 17:100912. https://doi.org/10.1016/j.animal.2023.100912.

Liinamo, A. E., P. Mäntysaari, and E. A. Mäntysaari. 2012. Short communication: Genetic parameters for feed intake, production, and extent of negative energy balance in Nordic Red dairy cattle. J. Dairy Sci. 95:6788–6794. https://doi.org/10.3168/jds.2012-5342.

Macrae, A. I., E. Burrough, J. Forrest, A. Corbishley, G. Russell, and D. J. Shaw. 2019. Prevalence of excessive negative energy balance in commercial United Kingdom dairy herds. Vet. J. 248:51–57. https://doi.org/10.1016/j.tvjl.2019.04.001.

McParland, S., and D. P. Berry. 2016. The potential of Fourier transform infrared spectroscopy of milk samples to predict energy intake and efficiency in dairy cows. J. Dairy Sci. 99:4056–4070. https://doi.org/10.3168/jds.2015-10051.

McParland, S., E. Kennedy, E. Lewis, S. G. Moore, B. McCarthy, M. O'Donovan, and D. P. Berry. 2015. Genetic parameters of dairy cow energy intake and body energy status predicted using mid-infrared spectrometry of milk. J. Dairy Sci. 98:1310–1320. https://doi.org/10.3168/jds.2014-8892.

Mehtiö, T., P. Mäntysaari, E. Negussie, A. M. Leino, J. Pösö, E. A. Mäntysaari, and M. H. Lidauer. 2020. Genetic correlations between energy status indicator traits and female fertility in primiparous Nordic Red Dairy cattle. Animal 14:1588–1597. https://doi.org/10.1017/S1751731120000439.

Meyer, K., and D. Houle. 2013. Sampling based approximation of confidence intervals for functions of genetic covariance matrices. Pages 523–526 in Proc. Assoc. Advmt. Anim. Breed. Genet. Vol. 20. N. Villalobos, ed. Napier, NZ. https://hdl.handle.net/1959.11/14324.

Misztal, I., K. Weigel, and T. J. Lawlor. 1995. Approximation of estimates of (co)variance components with multiple-trait restricted maximum likelihood by multiple diagonalization for more than one random effect. J. Dairy Sci. 78:1862–1872. https://doi.org/10.3168/jds.S0022-0302(95)76811-4.

Mota, L. F. M., D. Giannuzzi, S. Pegolo, E. Trevisi, P. Ajmone-Marsan, and A. Cecchinato. 2023. Integrating on-farm and genomic information improves the predictive ability of milk infrared prediction of blood indicators of metabolic disorders in dairy cows. Genet. Sel. Evol. 55:23. https://doi.org/10.1186/s12711-023-00795-1.

Oikonomou, G., G. Arsenos, G. E. Valergakis, A. Tsiaras, D. Zygoyiannis, and G. Banos. 2008. Genetic relationship of body energy and blood metabolites with reproduction in Holstein cows. J. Dairy Sci. 91:4323–4332. https://doi.org/10.3168/jds.2008-1018.

Paiva, J. T., R. R. Mota, P. S. Lopes, H. Hammami, S. Vanderick, H. R. Oliveira, R. Veroneze, F. Fonseca e Silva, and N. Gengler. 2022. Random regression test-day models to describe milk production and fatty acid traits in first lactation Walloon Holstein cows. J. Anim. Breed. Genet. 139:398–413. https://doi.org/10.1111/jbg.12673.

Pires, J. A. A., T. Larsen, and C. Leroux. 2022. Milk metabolites and fatty acids as noninvasive biomarkers of metabolic status and energy balance in early-lactation cows. J. Dairy Sci. 105:201–220. https://doi.org/10.3168/jds.2021-20465.

Ranaraja, U., K. H. Cho, M. N. Park, S. D. Kim, S. H. Lee, and C. H. Do. 2018. Genetic parameter estimation for milk β-hydroxybutyrate and acetone in early lactation and its association with fat to protein ratio and energy balance in Korean Holstein cattle. Asian-Australas. J. Anim. Sci. 31:798–803. https://doi.org/10.5713/ajas.17.0443.

Rustin, M., S. Janssens, N. Buys, and N. Gengler. 2009. Multi-trait animal model estimation of genetic parameters for linear type and gait traits in the Belgian warmblood horse. J. Anim. Breed. Genet. 126:378–386. https://doi.org/10.1111/j.1439-0388.2008.00798.x.

Smith, S. L., S. J. Denholm, M. P. Coffey, and E. Wall. 2019. Energy profiling of dairy cows from routine milk mid-infrared analysis. J. Dairy Sci. 102:11169–11179. https://doi.org/10.3168/jds.2018-16112.

Soyeurt, H., P. Dardenne, F. Dehareng, G. Lognay, D. Veselko, M. Marlier, C. Bertozzi, P. Mayeres, and N. Gengler. 2006. Estimating fatty acid content in cow milk using mid-infrared spectrom-

etry. J. Dairy Sci. 89:3690–3695. https://doi.org/10.3168/jds.S0022 -0302(06)72409-2.

Soyeurt, H., F. Dehareng, N. Gengler, S. McParland, E. Wall, D. P. Berry, M. Coffey, and P. Dardenne. 2011. Mid-infrared prediction of bovine milk fatty acids across multiple breeds, production systems, and countries. J. Dairy Sci. 94:1657–1667. https://doi.org/10.3168/ jds.2010-3408.

Stádník, L., F. Louda, and A. Jezkova. 2002. The effect of selected factors at insemination on reproduction of Holstein cows. Czech J. Anim. Sci. 47:169–175.

van der Drift, S. G. A., K. J. E. van Hulzen, T. G. Teweldemedhn, R. Jorritsma, M. Nielen, and H. C. M. Heuven. 2012. Genetic and non-genetic variation in plasma and milk β-hydroxybutyrate and milk acetone concentrations of early-lactation dairy cows. J. Dairy Sci. 95:6781–6787. https://doi.org/10.3168/jds.2012-5640.

Van Vleck, L. D. 1993. Selection index and Introduction to Mixed Model Methods for Genetic Improvement of Animals: The Green Book. CRC Press, Boca Raton, FL.

Varona, L., and O. González-Recio. 2023. *Invited review:* Recursive models in animal breeding: Interpretation, limitations, and extensions. J. Dairy Sci. 106:2198–2212. https://doi.org/10.3168/jds.2022 -22578.

Whitfield, R. G., M. E. Gerger, and R. L. Sharp. 1987. Near-infrared spectrum qualification via Mahalanobis distance determination. Appl. Spectrosc. 41:1204–1213. https://doi.org/10.1366/ 0003702874447572.

Wiggans, G. R., L. L. M. Thornton, R. R. Neitzel, and N. Gengler. 2006. Genetic parameters and evaluation of rear legs (rear view) for Brown Swiss and Guernseys. J. Dairy Sci. 89:4895–4900. https://doi.org/10 .3168/jds.S0022-0302(06)72538-3.

Xu, W., J. Vervoort, E. Saccenti, B. Kemp, R. J. van Hoeij, and A. T. M. van Knegsel. 2020. Relationship between energy balance and metabolic profiles in plasma and milk of dairy cows in early lactation. J. Dairy Sci. 103:4795–4805. https://doi.org/10.3168/jds.2019-17777.

Zachut, M., M. Šperanda, A. M. De Almeida, G. Gabai, A. Mobasheri, and L. E. Hernández-Castellano. 2020. Biomarkers of fitness and welfare in dairy cattle: Healthy productivity. J. Dairy Res. 87:4–13. https://doi.org/10.1017/S0022029920000084.

ORCIDS

Hongqing Hu, https://orcid.org/0000-0002-6408-1845
Sébastien Franceschini, https://orcid.org/0000-0001-6298-5149
Pauline Lemal, https://orcid.org/0000-0003-4937-0064
Clément Grelet, https://orcid.org/0000-0003-3313-485X
Yansen Chen, https://orcid.org/0000-0002-8593-4384
Hadi Atashi, https://orcid.org/0000-0002-6853-6608
Katrien Wijnrocx, https://orcid.org/0000-0001-5518-4933
Hélène Soyeurt, https://orcid.org/0000-0001-9883-9047
Nicolas Gengler https://orcid.org/0000-0002-5981-5509